

Research Paper

Comparative transcriptome analysis of *Fusarium graminearum* challenged with distinct fungicides and functional analysis of *FgICL* gene

Xuhao Guo^{a,b,1}, Kai He^{c,1}, Mengyu Li^{a,b,1}, Yuan Zhang^{a,b}, Jia Jiang^{a,b}, Le Qian^{a,b}, Xuheng Gao^{a,b}, Chengqi Zhang^d, Shengming Liu^{a,b,*}

^a College of Horticulture and Plant Protection, Henan University of Science and Technology, Luoyang 471023, China

^b Henan Engineering Technology Research Center of Green Plant Protection, Luoyang 471023, China

^c National Animal Protozoa Laboratory, College of Veterinary Medicine, China Agricultural University, Beijing 100193, China

^d College of Plant Protection, Anhui Agricultural University, Hefei 230036, China

ARTICLE INFO

ABSTRACT

Keywords:
Fusarium graminearum
 Fungicide
 RNA-seq
 Transcriptomic analysis
 Gene functional analysis

Fusarium graminearum is an economically important phytopathogenic fungus. Chemical control remains the dominant approach to managing this plant pathogen. In the present study, we performed a comparative transcriptome analysis to understand the effects of four commercially used fungicides on *F. graminearum*. The results revealed a significant number of differentially expressed genes related to carbohydrate, amino acid, and lipid metabolism, particularly in the carbendazim and phenamacril groups. Central carbon pathways, including the TCA and glyoxylate cycles, were found to play crucial roles across all treatments except tebuconazole. Weighted gene co-expression network analysis reinforced the pivotal role of central carbon pathways based on identified hub genes. Additionally, critical candidates associated with ATP-binding cassette transporters, heat shock proteins, and chitin synthases were identified. The crucial functions of the isocitrate lyase in *F. graminearum* were also validated. Overall, the study provided comprehensive insights into the mechanisms of how *F. graminearum* responds to fungicide stress.

1. Introduction

The homothallic *Fusarium graminearum*, one of the most economically important phytopathogenic fungi, is the dominant causal agent of Fusarium head blight (FHB) [1,2]. *F. graminearum* causes devastating disease on cereal crops worldwide, leading to tremendous loss of production and quality [2]. Due to climate change and shifts in agricultural systems, the prevalence of FHB has been more and more frequent and severe recently, with its appearance in regions where FHB has not been reported before [3,4]. Furthermore, over the past decade, the contamination of cereal grains by zearalenone, trichothecenes, and various other mycotoxins produced by *F. graminearum* has emerged as a growing global concern, posing significant threats to human and animal health [5,6]. In the group of trichothecenes, deoxynivalenol (DON) is the most worrisome mycotoxin in cereal grains worldwide, with a 59% average incidence rate [7]. Given that limited germplasm resource with effective and durable resistance to FHB is available in wheat, the chemical control is still the predominant approach to manage this disease in almost every

wheat-producing area. However, long-term application of chemical fungicides inevitably prompts the emergence of resistant strains in *F. graminearum* populations [8]. Therefore, it is of urgency to seek new ways to slow the expansion of resistance to fungicides in *F. graminearum*. Discovery of novel fungicides with new modes of action is one of the attempts to address this problem. Knocking down important genes resulted in significant inhibitory effects, indicating that essential genes could be used for *F. graminearum* control [9,10].

Carbendazim (CAR), a member of the class of benzimidazoles (MBCs), is widely used to control FHB in China for over forty years. It selectively binds to the β -tubulin monomer and disrupts the microtubule polymerization process, which leads to the arrest of microtubule formation and subsequently a failure in cell division [11,12]. Deletion of β_1tub increased resistance to carbendazim in *F. graminearum*, indicating that β_1tub gene affects the sensitivity to carbendazim [13]. Phenamacril (PHE) is an effective Fusarium-specific fungicide for controlling FHB. *FgMyo1*, a class I myosin of *F. graminearum*, was reported to be the target of phenamacril and a point mutation in *FgMyo1* could result in

* Corresponding author.

E-mail address: liushengmingzb@163.com (S. Liu).

¹ These authors contributed equally to the work.

F. graminearum resistance to phenamacril [14]. However, some studies suggested other proteins also affect the sensitivity to phenamacril in *F. graminearum* [10,15]. Pyraclostrobin (PYR) which belongs to the quinone outside inhibitor (QoI) class, is a commonly used fungicide to control various plant diseases. The QoI fungicide acts by blocking electron transport at the quinol-oxidizing site of the cytochrome bc1 complex in the mitochondrial respiration chain, effectively inhibiting ATP synthesis [16]. The point mutation found in *cytb* gene has been reported as the main mechanism causing high resistance to QoI fungicides [17,18]. Tebuconazole (TEB), a sterol demethylation inhibitor (DMI), has been pivotal in managing FHB for over two decades. DMIs like tebuconazole hinder ergosterol biosynthesis in fungi by interacting with cytochrome P450 sterol 14 α -demethylase (CYP51) [19,20]. Depletion of ergosterol disrupts cell membrane function, impeding fungal growth [21]. However, DMI resistance is rising, marked by mutations in CYP51 genes, gene overexpression [22], and increased activity of efflux pumps [23]. In wheat fields, DMI-resistant strains of *F. graminearum* have been identified, though no mutations in CYP51 genes were detected, and no correlation with gene expression was observed [20].

Since the genome of the filamentous fungus *F. graminearum* was sequenced and annotated, it has provided fundamental basis for future work [24]. A growing body of research using transcriptomics, proteomics, and metabolomics has been established to explore pathogenesis, reproduction, and host defense mechanism of *F. graminearum* [25–28]. With most of sequencing methods have become more affordable and feasible over the past years, many studies have taken advantages of RNA-seq to identify genes with a potential role in the biological responses to stress in microorganisms [29–31]. However, comparative analyses of *F. graminearum*'s global transcriptional responses to diverse fungicidal stresses are scarce, and the downstream implications for cellular pathways remain largely obscure. Hence, this study aims to fill the existing gap by profiling the transcriptomic changes in *F. graminearum* when challenged with four distinct fungicides (carbendazim, phenamacril, pyraclostrobin, and tebuconazole) using RNA-seq. Further investigation identified some key genes in response to different stresses and revealed their pleiotropic phenotypes. The results would help to contribute to the current knowledge of how fungi react with fungicides with different mechanism of action and provide valuable resources for uncovering novel antifungal targets in *F. graminearum*.

2. Materials and methods

2.1. Strains, media and fungicides

The *Fusarium graminearum* strain AY1801 used in this study was collected from a wheat field in Henan, China. It was single spore isolated and continued incubated on potato sucrose agar medium (PSA, 200 g of potato, 16 g of agar, and 20 g of sucrose per liter of distilled water) at 25 °C in the dark for use. Mung bean soup medium (MS, mung bean 30 g per liter of distilled water) was used to obtain spores while YEPD medium (0.3% of yeast extract, 2% of dextrose and 1% of peptone per liter of the distilled water) was used for the fungicide treatment test. The spore germination assay was conducted on water agar medium (WA, 16 g of agar per liter of distilled water) and the assay of utilization of different carbon sources was tested on minimal medium (0.5 g of KCL, 0.5 g of MgSO₄ 7H₂O, 1 g of KH₂PO₄, 2 g of NaNO₃, 0.01 g of FeSO₄ 7H₂O, 30 g of sucrose per liter of distilled water). Technical grade carbendazim (MBC, 98%) was provided by Jiangsu Rotam Chemistry Co. Ltd. (Suzhou, China), phenamacril (95%) was generously supplied for free by Jiangsu Pesticide Research Institute Co. Ltd. (Nanjing, China), pyraclostrobin (97.5%) and salicylhydroxamic acid (SHAM, 99%) was provided by Nanjing Agricultural University, and tebuconazole (98%) was provided by Hunan Bide Biochemical Technology Co. Ltd. (Yueyang, China). The carbendazim was dissolved in 0.1 M hydrochloric acid and phenamacril, pyraclostrobin, and tebuconazole were each

dissolved in methanol respectively for using and stored at 4 °C.

2.2. Sensitivity determination

The effective concentration for 50% inhibition of mycelial growth (EC₅₀) of strain AY1801 to carbendazim, phenamacril, pyraclostrobin, and tebuconazole was determined using method of mycelial growth rate described previously [32]. Three-day old mycelial plugs (5 mm) from the edge of the colony were transferred onto PSA medium plates (9 cm) containing a series of concentrations of the four fungicides as follows: carbendazim, 0.3, 0.5, 0.7, 0.9, 1.1 µg/mL, phenamacril, 0.0625, 0.125, 0.25, 0.5, 1 µg/mL, pyraclostrobin, 0.125, 0.25, 0.5, 1, 2 µg/mL, and tebuconazole, 0.1, 0.2, 0.4, 0.6, 0.8 µg/mL. PSA Plates amended without fungicides were used as controls. Sensitivity tests for pyraclostrobin were carried out with the addition of SHAM, a specific inhibitor of alternative oxidase [33], at a final concentration of 100 µg/mL for each treatment. After incubation for 3 days at 25 °C in the dark, the diameters of each colony were measured in two perpendicular directions. The inhibition rate of mycelia growth was calculated using the formula: inhibition rate = (control colony diameter – treated colony diameter) / (control colony diameter – 5 mm) × 100%. The EC₅₀ value was calculated by linear regression of relative percentage of growth inhibition against log-transformed fungicide concentration. Statistical analysis was performed using Data Processing System software (DPS, version 7.05, Zhejiang University, Hangzhou, China).

2.3. RNA extraction, cDNA library construction and sequencing

Ten mycelial plugs (diameter = 5 mm) from the strain AY1801 at the growing edge of the colony were transferred into a flask containing 100 mL of 3% MS medium and shaken at 150 rpm and 25 °C for 7 days under a 12 h photoperiod. The spores collected with filter papers were then measured for the amount of conidia under a microscope using a hemocytometer and the solution was diluted to 5 × 10⁴ spores/mL. Subsequently, 1 mL of spore solution was transferred into flasks containing 100 mL of YEPD media and incubated on a shaker at 150 rpm and 25 °C for 24 h in the dark. After the spores fully germinated, carbendazim, phenamacril, pyraclostrobin, and tebuconazole were added into the flasks at 2 × EC₅₀ concentration respectively and those without fungicides were considered as a control. After 7 days of culturing under the same conditions, the fresh mycelia including three independent biological replicates of each treatment group was centrifuged and collected for RNA extraction with Trizol reagent (Takara) according to the manufacturer's instructions. The RNA quality was determined by 2100 Bioanalyzer (Agilent Technologies) and quantified by ND-2000 (Nano-Drop Technologies). Thereafter, the high-quality RNA samples were used for the subsequent cDNA synthesis, terminal repair and ligation of Illumina sequencing adaptors according to the manufacturers' protocol. After quantification using the TBS380 mini-fluorometer system (TurnerBio Systems, Inc. USA), all constructed libraries were sequenced by the Illumina NovaSeq 6000 sequencer with a paired-end strategy (2 × 150 bp).

2.4. Data processing, differential expression analysis, and functional annotation

For the sequencing data, the raw paired end reads were trimmed and quality controlled by fastp software (v0.21) with default parameters. All the acquired clean reads were then mapped against the reference genome: *Fusarium graminearum* PH-1 (assembly ASM24013v3, https://www.ncbi.nlm.nih.gov/datasets/genome/GCF_000240135.3/ graminearum) using Hisat2 (v2.0.5) [34]. RSEM (RNA-Seq by Expectation-Maximization) v1.3.3 was used to quantify the raw count of each gene, with gene expression levels being evaluated based on the transcripts per million reads (TPM) method. Differential expression genes (DEGs) were identified by calculating the expression level of each gene using the

DESeq2 (v1.42.0) [35]. The significance threshold for the differential expression was set at an FDR (false discovery rate) < 0.05 and a $|\log_2 \text{fold change}| > 1$. All DEGs from the four comparison groups were combined to assess the gene expression pattern variations among the different treatments based on the fuzzy C-Means clustering algorithm using 'Mfuzz' package in R (v4.0). Additionally, GO and KEGG enrichment analysis were carried out by the 'clusterProfier' package (v4.5.2) in R (v4.0). The GO terms and KEGG pathways were considered to be significantly enriched as the P -value < 0.05 using the method of Fisher's exact test.

2.5. Weighted gene co-expression network analysis (WGCNA)

Weight gene co-expression network analysis (WGCNA) for these DEGs was conducted using the 'WGCNA' package (v1.72.5) to identify specific modules of co-expression genes associated with each treatment [36]. Prior to WGCNA, genes with low expression (mean TPM value of all samples ≤ 1) were excluded to improve the accuracy of the resulting network. To identify biologically significant modules, a co-expression network was constructed with a beta value of 14. Subsequently, gene expression modules with similar patterns were identified based on gene cluster dendrogram using the dynamic tree cut method (minModuleSize = 30 and mergeCutHeight = 0.4). The five groups were used as the traits to calculate correlation coefficients with module eigengenes. Module with an absolute correlation coefficient > 0.85 and P -value < 0.05 was defined a key module. The gene connectivity in module were calculated by the 'intramodularConnectivity' function in WGCNA package. Hub genes were identified as those with most connections and correlation in the network, as indicated by their high Module Membership (MM) and Gene Significance (GS) value ($|\text{MM}| > 0.8$ and $|\text{GS}| > 0.2$).

2.6. Quantitative real-time PCR

All the RNA extracted from the sample as described above was synthesized into cDNA by reverse transcription using the PrimeScript RT reagent Kit with gDNA Eraser (Takara). The expression level of *FgICL* and eight randomly selected genes in treatment group and control was quantified by quantitative real-time PCR with TB Green® Premix Ex Taq (Takara) (Table S1). The *ef1α* gene (FGSG_08811) was used as reference gene for the calculation of expression level of target genes. Relative gene expression levels were analyzed using the $2^{-\Delta\Delta CT}$ method. All reactions were performed with three biological replicates.

2.7. Generation of gene deletion and complementation mutants

The *FgICL* gene deletion mutants were generated using the homologous recombination approach as previously described [37]. Briefly, the 939 bp upstream and 972 bp downstream flanking fragments of *FgICL* gene were amplified from the genomic DNA of strain AY1801, respectively. The hygromycin phosphotransferase (hph) gene and the thymidine kinase gene from the herpes simplex virus 1 (hsv), which confers resistance to the antibiotic hygromycin and sensitivity to nucleoside analog 5-Fluoro-2'-deoxyuridine, were amplified from pKHT plasmid. Subsequently, these fragments were fused by double-joint PCR to construct the replacement cassette as previously described [38]. The resulting cassette were transformed into protoplasts of strain AY1801 as previously described [39]. After transformation, hygromycin-resistant transformants selected in the presence of 5-Fluoro-2'-deoxyuridine were first screened by PCR to confirm the *FgICL* gene deletion and further confirmed by RT-qPCR. For complementation, the fragment containing the full *FgICL* gene was amplified from the genomic DNA of strain AY1801. The resulting cassette were transformed into protoplasts of strain $\Delta Fgicl-1$. Similarly, the transformants were screened with hygromycin and 5-Fluoro-2'-deoxyuridine and further confirmed by PCR and RT-qPCR. The primers used in this section are listed in Table S1.

2.8. Functional characterization of *FgICL* gene

To measure the spore production capability, 10 fungal discs taken from the edge of a PDA plate cultured for 4 days were inoculated into 100 mL mung bean broth medium in conical flasks and placed on a shaker at 28 °C, 180 rpm, with a 12-h light/12-h dark cycle. After 7 days, the spores were collected and the spore production for each strain was counted using a hemocytometer, with three replicates per strain. Subsequently, the spore germination assay was conducted. Suspensions of spores for each strain were prepared, and 0.2 mL of the spore suspension was spread evenly on a WA plate using a spreader. The plates were incubated at 25 °C for approximately 6 h. Spore germination of the wild-type strain was observed under a microscope (germination defined as the length of the germ tube exceeding half of the spore length). Once the wild-type strain showed a germination rate of over 90%, the spore germination rates of various mutants were recorded. The sensitivity of the strains to fungicides was tested by the method of mycelial growth rate described above. To assess the stress response capability of the mutants, all strains were inoculated on PDA plates containing 1 mol/L NaCl, 1 mol/L KCl, 5 mmol/L H₂O₂, 0.1 g/L SDS, and 0.1 g/L Congo Red. For the assay of utilization of different carbon sources, all strains were inoculated on MM media without carbon source, with 3% glucose, 3% fructose, 3% mannose, 3% sucrose, and 3% galactose, respectively. After 4 days of incubation, the colony diameters of each strain were measured to determine their response to ion stress and assess their utilization of different carbon sources. Three replicates were set for each strain, and these experiments mentioned above were repeated three times.

3. Results

3.1. Sensitivity determination

The sensitivity of *F. graminearum* strain AY1801 to carbendazim, phenamacril, pyraclostrobin, and tebuconazole was determined by mycelial growth rate. Results showed that the EC₅₀ values of AY1801 to carbendazim, phenamacril, pyraclostrobin, and tebuconazole were 0.594 µg/mL, 0.174 µg/mL, 0.097 µg/mL, and 0.165 µg/mL, respectively (Fig. 1). Based on the EC₅₀ value of AY1801 to the four fungicides, twofold dose EC₅₀ of 1.188 µg/mL of carbendazim, 0.348 µg/mL of phenamacril, 0.194 µg/mL of pyraclostrobin, and 0.330 µg/mL of tebuconazole were used to treat strain AY1801 for further study.

3.2. Overall RNA analysis of *F. graminearum* responding to the four fungicides

To understand the diverse transcriptional adaptations of *F. graminearum* to different fungicides, we utilized RNA-seq to unveil transcriptome-wide changes triggered by four distinct chemical challenges. After quality control filtering of high-throughput sequencing, a total of 102G clean reads from 15 RNA-seq libraries were obtained with an average of 6.85G clean data sequenced per library, of which 95.56% were mapped onto the reference genome of *F. graminearum* on average (Table S2). Principal component analysis (PCA) analysis showed the consistency between the three biological replicates with high correlation in the same group (Fig. 2A), which were divided by PC1 (54.9%) and PC2 (14.3%). Additionally, the correlation heatmap of all samples also revealed the clear clustering pattern of replicates samples, except for one replicate from the control group (Fig. S1A). The following analysis displayed the distribution of gene expression levels for all samples based on the TPM method, with details on expression values and annotations recorded (Fig. S1B). Subsequently, we conducted pairwise comparisons between control and each fungicide-treated groups to further elucidate the specific effects of these fungicides. A total of 8019 DEGs from the four treatments were confirmed by 'DESeq2' package ($\log_2 \text{FC} > 1$, $P\text{-adjust} < 0.05$) when compared with the control group. Specifically, 5086, 2559, 5680 and 3182 DEGs were identified in the CAR vs. CK, PHE

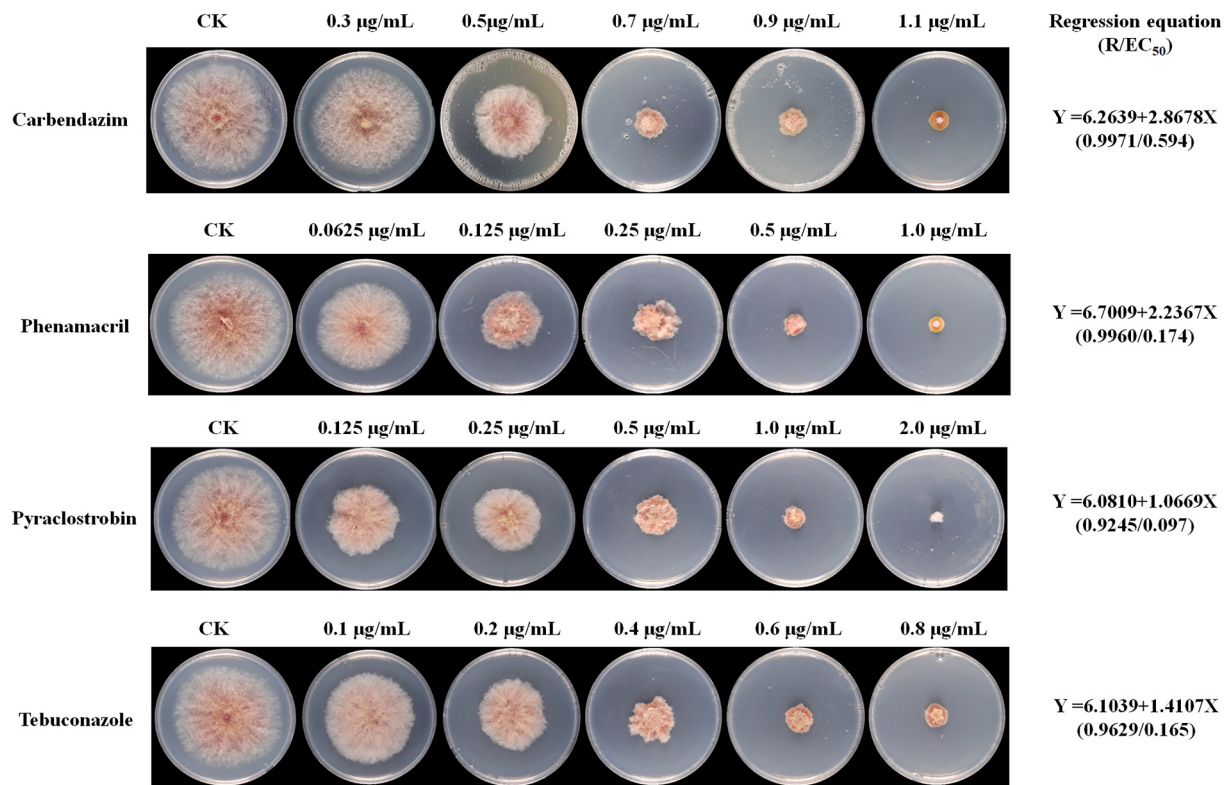


Fig. 1. Sensitivity of *F. graminearum* against carbendazim, phenamacril, pyraclostrobin, and tebuconazole was determined by mycelial growth rate.

vs. CK, PYR vs. CK and TEB vs. CK comparison sets, respectively (Fig. 2B). Venn diagrams further showed that 756 (269 up- and 487 down-regulated) DEGs were common across all four treatments, and more group-specific genes were identified in the PYR (1371 genes) and TEB (963 genes) than in the CAR (799 genes) and PHE (576 genes) (Fig. 2C and D). Notably, intersections between these DEG sets showed that PYR treatment exhibited the largest number of changes for both up- and down-regulation.

3.3. Functional annotation and enrichment of DEGs

To elucidate the functions of these DEGs, we compared the DEGs from the four treatment groups with the Gene Ontology (GO) database. They were subsequently categorized into three types of biological processes (BP), cellular components (CC), and molecular functions (MF). The annotated results demonstrated that the highest number of DEGs were enriched in three key categories: “metabolic process,” “membrane part,” and “catalytic activity” (Fig. S2). Furthermore, GO enrichment analysis was separately conducted for the identified up- and down-regulated DEGs mentioned above. A comparison was made to assess whether the associated biological functions were common or group-specific (Fig. 2E and F). Interestingly, both up- and down-regulated DEGs in CAR treatment exhibited functional similarity to PYR treatment and appeared to display stronger responses than the other two fungicides. For instance, the enrichment results unveiled that up-regulated genes were predominantly associated with carbohydrate, cellular lipid and oxoacid metabolism, and macromolecule biosynthetic processes. In contrast, down-regulated genes were implicated in processes related to endonucleolytic cleavage and maturation of rRNA under the two treatments. Moreover, genes associated with the nitrogen compound metabolic process exhibited significant down-regulated in the CAR and PYR group, and genes related to the term of DNA repair was consistently down-regulated under the treatment of PHE and TEB. Notably, there was no shared GO term between them, indicating distinct responsive mechanisms among the four fungicides.

Through functional annotation of these DEGs using the EggNOG database, a total of 1642, 963, and 746 genes from the four comparison sets were mapped to known functional classifications related to “metabolism,” “cellular processes,” and “signaling and information storage and processing,” respectively (Fig. 3A). It’s noteworthy that nearly half of the annotated genes were associated with carbohydrate, amino acid, and lipid transport and metabolism. To delve deeper into metabolic pathways, we categorized DEGs into five groups using the KEGG databases (Fig. 3B). The dot plot confirmed the primary KEGG metabolic annotations of DEGs from the four comparison sets at the first two KEGG levels (Fig. S2), which could be classified into five basic categories. Obviously, these categories were further divided into 20 subcategories, with the largest number of subclasses identified in the “Metabolism” category. From top to bottom, the most abundant DEGs in both comparisons were associated with carbohydrate and amino acid metabolism, which further reflect the consistency observed in different databases (see details in Table S3). Simultaneously, KEGG enrichment analyses were conducted to show the top 20 significantly enriched metabolic pathways ($P < 0.05$) in the four comparisons (Fig. 4). Among these pathways, some central carbon pathways were observed to occur in all treatment groups, such as Glycolysis/Gluconeogenesis, Citrate cycle, and Pentose phosphate pathway, indicating potential overlapping transcriptional responses when *F. graminearum* was exposed to various fungicides. Additionally, steroid biosynthesis was also notably enriched in the TEB treatment group as anticipated.

3.4. Dynamic transcriptomic profiles among the different fungicides

Furthermore, C-means clustering based on fuzzy c-mean algorithms were performed to identify the transcripts that might contribute to the fungicide stress responses across the four treatments. The expression levels of the combined 8109 DEGs were grouped into eight clusters and plotted by a heatmap. The heatmap showed a quite different transcriptome profiles, demonstrating the varied responsive patterns during the interactions of *F. graminearum* and the four fungicides (Fig. 5).

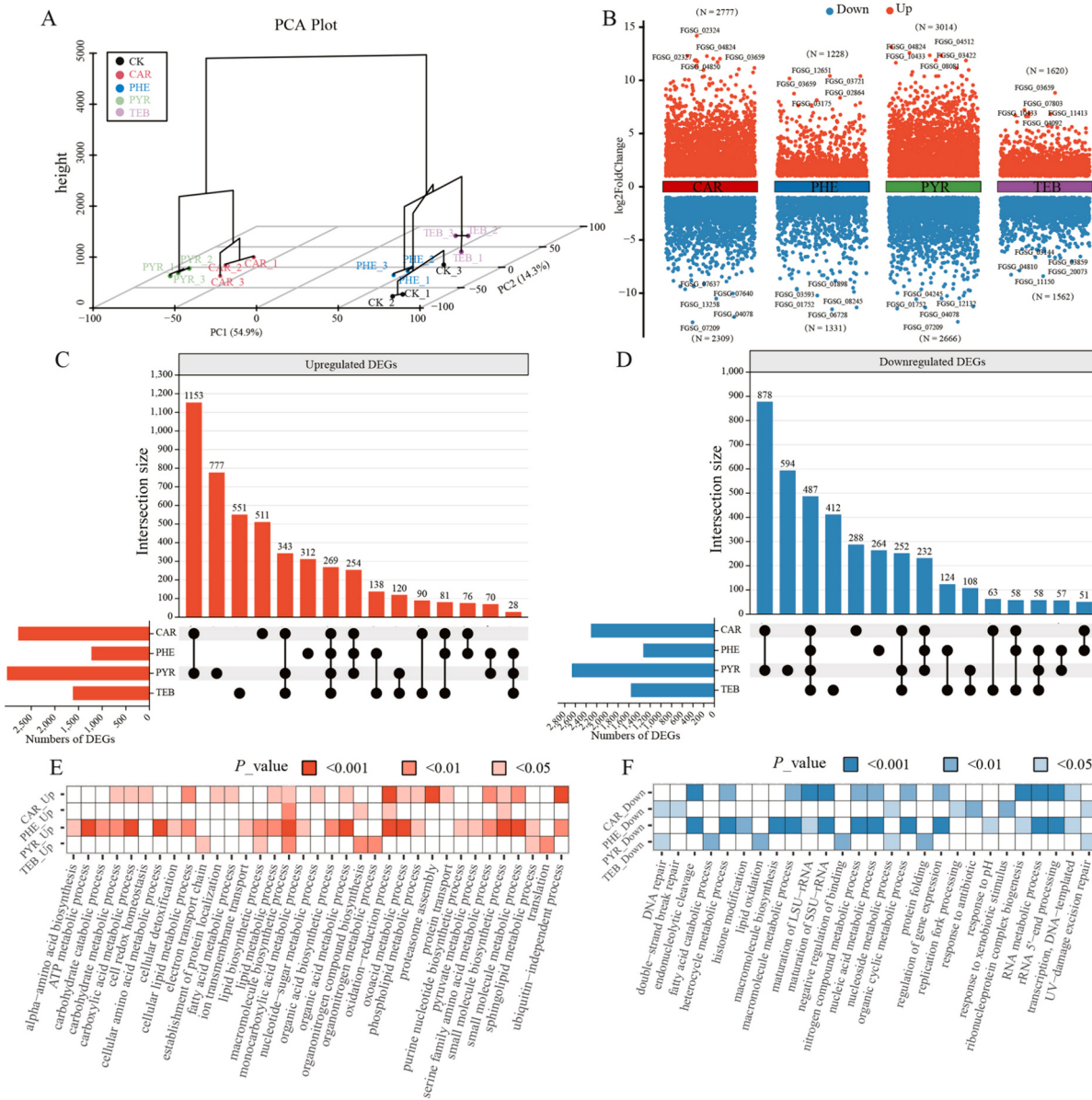


Fig. 2. Transcriptome profiles of *F. graminearum* in response to carbendazim, phenamacril, pyraclostrobin, and tebuconazole. (A) Principal component analysis (PCA) was performed to show the consistency between three biological replicates. (B) Scatter plot showing the number of DEGs across the four comparison groups, where the red points represent the up-regulated genes and the green points represent the down-regulated ones. (C and D) Upset plots of upregulated (C) and downregulated (D) DEGs and their overlap between treatments. The bottom left horizontal barplot show the total number of DEGs identified in each fungicide. The top barplot summarizes the number of DEGs for each unique or overlapping combination as indicated by the connecting circles below. (E and F) Gene Ontology (GO) enrichment analysis of upregulated (E) and downregulated (F) DEGs in each treatment. The selected significant GO terms of each treatment are shown. The color intensity in both panels denotes illustrates the significance, where red/blue indicates a higher degree of enrichment. (For interpretation of the references to color in this figure legend, the reader is referred to the web version of this article.)

Among these clusters, cluster 1, 4, 5 and 8 were of particular interest, since genes in the four clusters showed a dramatic increase under PYR, TEB, PHE, and CAR treatment, respectively. This alignment with previous results suggests that the increased activity in these functions is attributed to the elevated expression of specific genes under the corresponding treatments, aiding in the identification of targets for various fungicides. Notably, in addition to cluster 1 and 5, Glyoxylate and dicarboxylate metabolism were also found to occur in the enrichment results of cluster 6. It's obvious that the transcript levels of genes involved in the pathway were significantly increased, with the exception of those treated with TEB. Consistently, KEGG results also showed that TCA cycle was significantly activated under the treatment of CAR, PHE and PYR group, implying that these related DEGs may contribute to the

TCA cycle through Glyoxylate cycle.

By mapping these expression profiles to the KEGG database, we observed a clear discrepancy in the expression levels of DEGs involved in Glycolysis/Gluconeogenesis, the TCA cycle, and the Glyoxylate cycle. (Fig. 6 and S3). In fact, none of genes in the TCA pathway were significantly altered by TEB treatment. Therefore, we further focused on the DEGs involved in carbohydrate metabolism that were significantly altered in all treatments, except for TEB (Table 1). We found that most of these genes were from the cluster 6 and mostly link to Glycolysis and TCA cycle. These genes include *FGSG_06619* (*ADH6*, EC:1.1.1.2), *FGSG_12857* (*ACL1*, EC: 2.3.3.8), *FGSG_06039* (*ACL2*, EC: 2.3.3.8), *FGSG_04309* (*ODO1*, EC: 1.2.4.2) and *FGSG_02461* (*MDH1*, EC: 1.1.1.37). Notably, two genes encoding isocitrate lyase (*FGSG_09896*



Fig. 3. Functional classification and annotation targeting to COG and KEGG databases based on the identified DEGs. (A) The number and percent of known annotated genes involved in metabolism, cellular processes and signaling, and information storage and processing in the EggNOG database. (B) The dot plot showing the annotated pathways at the top two levels of KEGG database.

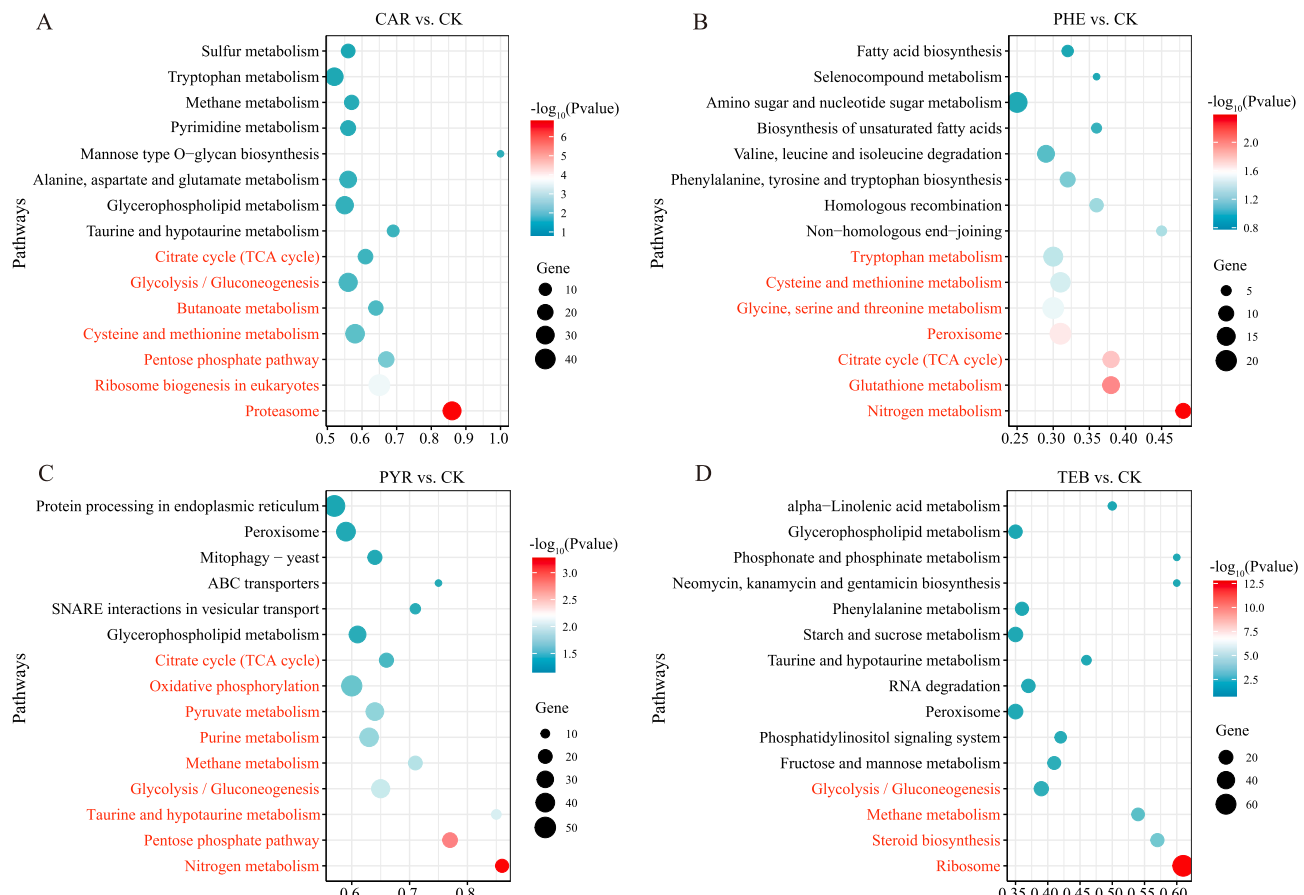


Fig. 4. Kyoto Encyclopedia of Genes and Genomes (KEGG) enrichment of DEGs in the four treatment groups. The top 15 non-redundant pathways of each group are shown. The pathways marked in red denotes the significance in statistics ($P < 0.05$). (For interpretation of the references to color in this figure legend, the reader is referred to the web version of this article.)

and FGSG_00176 EC:4.1.3.1) of *F.graminearum* in the glyoxylate cycle exhibit the different response, whereas only FGSG_09896 (*FgICL*) appear to markedly change in all groups except TEB group.

In addition, as shown in Table S4, we also found significant changes in the expression levels of key DEGs associated with ATP-binding cassette (ABC) transporters, heat shock proteins (HSP), and chitin synthases (CHS). Briefly, 14 ABC transporters, 9 HSPs and 7 CHSs were defined as the DEGs upon at least one fungicide treatment. Taken together, these results suggested these genes associated with stress response may participate in the process of *F. graminearum* answering fungicide stress.

3.5. Co-expression gene network analysis of DEGs and identification of hub genes

To further understand the global transcriptional organization underlying fungicides responses and interspecific divergence, we applied the weighted gene co-expression network analysis (WGCNA) analysis of the joint DEGs from the four comparisons. Firstly, to ensure the network was scale-free and exhibited greater biological significance, the optimal soft threshold was set as 14 (Fig. 7A). As displayed in Fig. 7B, 11 gene modules were ultimately generated after merging. Eigengene dendrogram and eigengene adjacency were plotted to dissect the connectivity of module eigengenes (MEs), and the results showed that the distance between modules was >0.4 .

The module-trait correlation coefficients were calculated and the results were shown in Fig. 7C. Interestingly, ME2 with 871 genes, ME4 with 2183 genes, ME6 with 1611 genes, and ME9 with 613 genes showed a significant positive correlation with gene expression profiles of

CAR, PYR, PHE and TEP treatments ($|R| \geq 0.85$ and $P < 0.05$), respectively. Therefore, the four modules were further examined to characterize the co-expression dynamics and functional association. According to the criteria of $|GS| > 0.2$ and $|MM| > 0.8$, a total of 401, 1308, 275 and 270 crucial genes that are highly associated with the expression profile of each treatment were identified from the above four modules (Fig. S4A-D). Functional enrichment analysis was performed on the hub genes identified in the four modules to discern their roles in metabolic pathways (Fig. S4E). Similarly, pentose phosphate pathway, glycolysis/gluconeogenesis, citrate cycle and steroid biosynthesis were markedly enriched in the ME2, 4, 6 and 9, respectively. To some extent, the enrichment results from the modules showed some similarity to those of Cluster 8, 1, 5, and 4. Considering this, these results suggest that central carbon pathways are indeed markedly affected by the three fungicides except TEB treatment.

3.6. Validation of RNA-seq data

To validate the RNA-seq results, *FgICL* and other 8 randomly selected DEGs were used for qRT-PCR analysis via gene-specific primers. The relative expression level changes of each gene in the different groups were detected with similar trends using both methods (Fig. 8). These results confirmed that the RNA-seq data is reliability and convincing.

3.7. Functional analysis of *FgICL* gene

To study the function of *FgICL* gene, we generated deletion mutants using a homologous recombination strategy and confirmed three *FgICL* deletion mutants $\Delta Fgicl-1$, $\Delta Fgicl-2$, and $\Delta Fgicl-3$. Furthermore, the *FgICL*

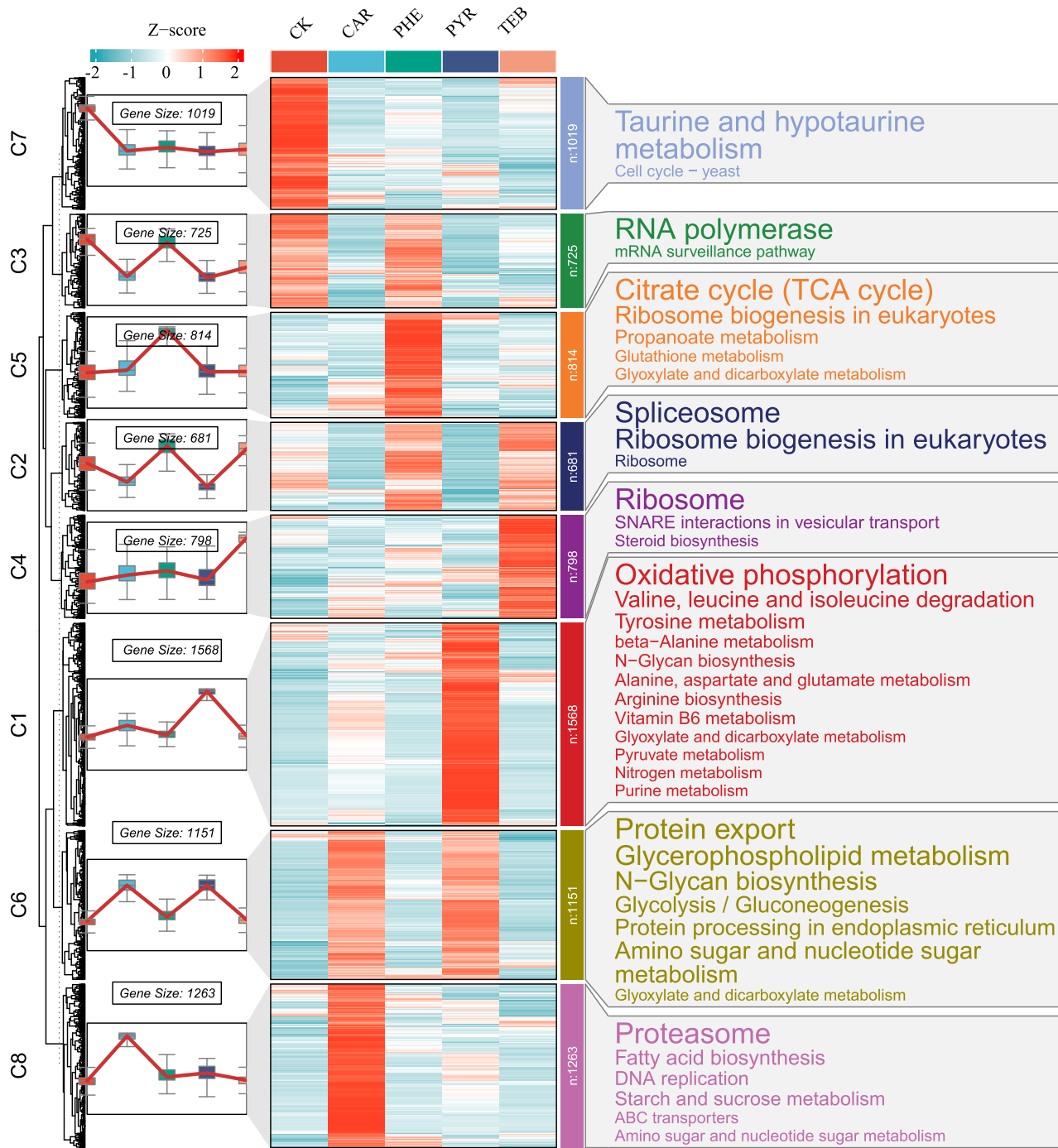
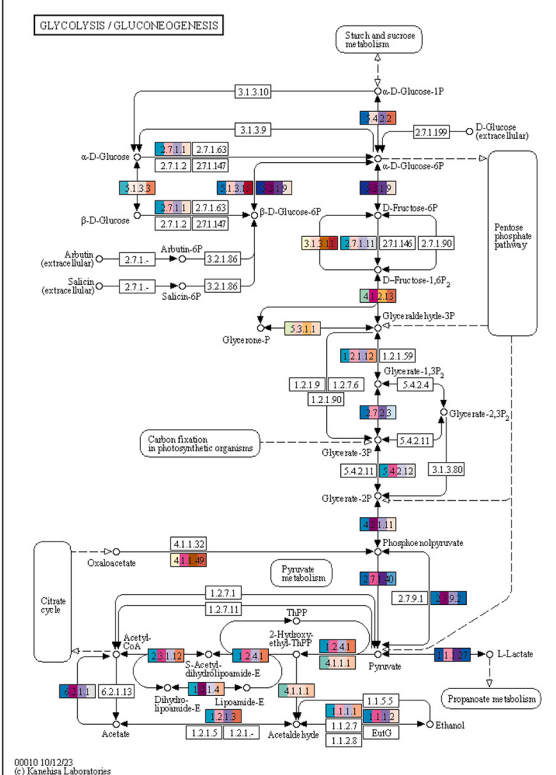


Fig. 5. Transcriptomic variation tendencies and responsive dynamics among the different fungicides. The gene clustering heatmap and trend diagram indicate the different expression patterns, the corresponding KEGG enrichment results are displayed on the right-hand side.

gene with its native promoter was reintroduced into the protoplast of $\Delta FgICL-1$, resulting in the complemented strain $\Delta FgICL-C$ (Fig. S5). The strains of AY1801, $\Delta FgICL-1$, $\Delta FgICL-2$, $\Delta FgICL-3$, and $\Delta FgICL-C$ were used for further phenotype analyses. Although there was no significant difference in sporulation ability, the spore germination rate of the $FgICL$ gene deletion mutants were significantly lower than that of the wild-type strain. Complementation of the $FgICL$ gene rescued this defect (Fig. 9A and B, Fig. S6), suggesting that the $FgICL$ gene is involved in the spore germination process of *F. graminearum*. The lesion length on wheat coleoptiles infected by $\Delta FgICL-1$ and $\Delta FgICL-3$ strains was significantly lower than that of the wild-type strain and $\Delta FgICL-C$ strain (Fig. 9C), indicating that deletion of the $FgICL$ gene reduces the ability of *F. graminearum* to

infect wheat. In terms of ion stress tolerance, under potassium ion stress, the growth rate of the $FgICL$ gene deletion mutants was significantly reduced (Fig. 9D, Fig. S6). However, deletion of the $FgICL$ gene didn't affect the growth of *F. graminearum* under hydrogen peroxide, Congo red or SDS (Fig. 9D, Fig. S6). These results suggest that the $FgICL$ gene may be involved in *F. graminearum*'s response to ion stress, but not to oxidative, cell wall and membrane stress. Regarding the utilization of different carbon sources, although there was no difference in growth rate on glucose- and galactose-containing MM media, the growth rate of the $FgICL$ gene deletion mutants was significantly reduced on mannose, fructose, and sucrose-containing MM media (Fig. 9E), indicating that the absence of the $FgICL$ gene affected the utilization of different carbon

A



B

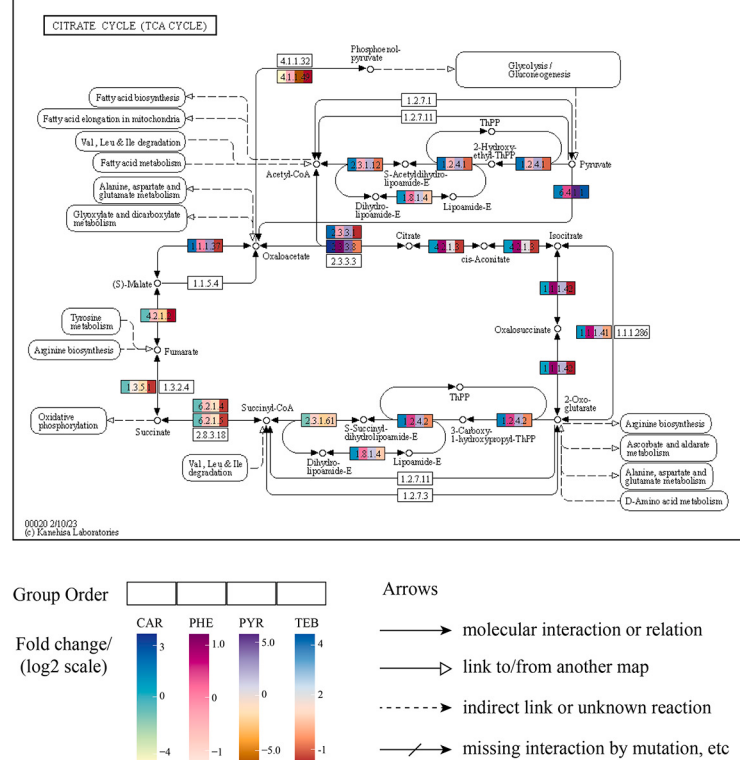


Fig. 6. KEGG pathway mapping analysis of (A) glycolysis/gluconeogenesis (fgr:00010) and (B) citrate cycle (TCA cycle) (fgr:00020) based on the DEGs induced by the four fungicides. The changes of color inside the boxes represent the alteration of gene expression level in CAR vs. CK, PHE vs. CK, PYR vs. CK and TEB vs. CK, respectively.

Table 1

Alterations of gene expression for the identified key DEGs related to Carbohydrate metabolism.

Gene	Name	Description	Log2FC (Treatment vs. CK)				Cluster
			CAR	PHE	PYR	TEB	
FGSG_03212	CHIA1	Chitinase A1	3.28*	1.96*	3.2*	1.09	6
FGSG_01199	GFA1	glucosamine-fructose-6-phosphate aminotransferase	1.89*	2.32*	1.87*	-0.53	5
FGSG_06039	ACL2	ATP-citrate synthase subunit 2	3.07*	2.51*	2.63*	-0.75	6
FGSG_12857	ACL1	ATP-citrate synthase subunit 1	4.01*	2.15*	3.7*	0.12	6
FGSG_04309	ODO1	2-oxoglutarate dehydrogenase	1.03*	1.55*	1.35*	-0.25	5
FGSG_02461	MDH1	malate dehydrogenase	2.76*	1.07*	3.08*	-0.5	6
FGSG_06619	ADH6	alcohol dehydrogenase (NADP+)	2.63*	1.1*	3.03*	0.95	6
FGSG_09896	ICL1	isocitrate lyase	1.83*	1.48*	1.67*	-0.57	6
FGSG_01279	GSDA	Glucose-6-phosphate 1-dehydrogenase	1.24*	1.1*	1.32*	-0.96	6
FGSG_09643	FOX-2	peroxisomal hydratase-dehydrogenase-epimerase	4.19*	1.51*	1.66*	-0.73	8
FGSG_05284	HIBA	3-hydroxyisobutyrate dehydrogenase	4.22*	1.92*	5.29*	0.98	1
FGSG_06580	ACAC	acetyl-CoA carboxylase	4.66*	1.47*	2.96*	-0.93	8
FGSG_09321	ERG10	acetyl-CoA acetyltransferase IB	3.56*	1.5*	3.64*	-0.2	6
FGSG_09366	EGLC	glucan- β -glucosidase	2.67*	1.13*	3.13*	0.69	6
FGSG_11777	-	Hypothetical protein	4.36*	2.34*	3.22*	0.69	8

The symbol “*” represent the significantly changed DEGs in the comparison group.

sources by *F. graminearum*. Compared with the wild-type strain, three deletion mutants showed significantly increased sensitivity to tebuconazole (Fig. 9F, Fig. S6), implying that *FgICL* gene is involved in the process of *F. graminearum* coping with fungicides.

4. Discussion

The ongoing advancement of high-throughput technologies has not only facilitated the publication and optimization of the *F. graminearum* genome but has also significantly spurred the elucidation of mechanisms for coping with fungicide stress and the adaptation of fungicides, achieving unprecedented precision. In two independent studies, the

transcriptional response of *F. graminearum* to tebuconazole was explored by deep serial analysis of gene expression (DeepSAGE) sequencing approach and novel microarray respectively, providing useful information in the understanding of the mechanisms for the response of *F. graminearum* to tebuconazole [26,29]. It is well known that the continued large-scale use of fungicides of single mode may increase the risk of FHB outbreak, so there is still a need to evaluate the effects of diverse fungicides in more details. In the current study, we used RNA-seq to systematically outline the transcriptomic changes of *F. graminearum* treated by four fungicides with different mechanisms. The results revealed key genes, pathways associated with fungicide response in *F. graminearum*, enhancing our understanding of the regulatory genes

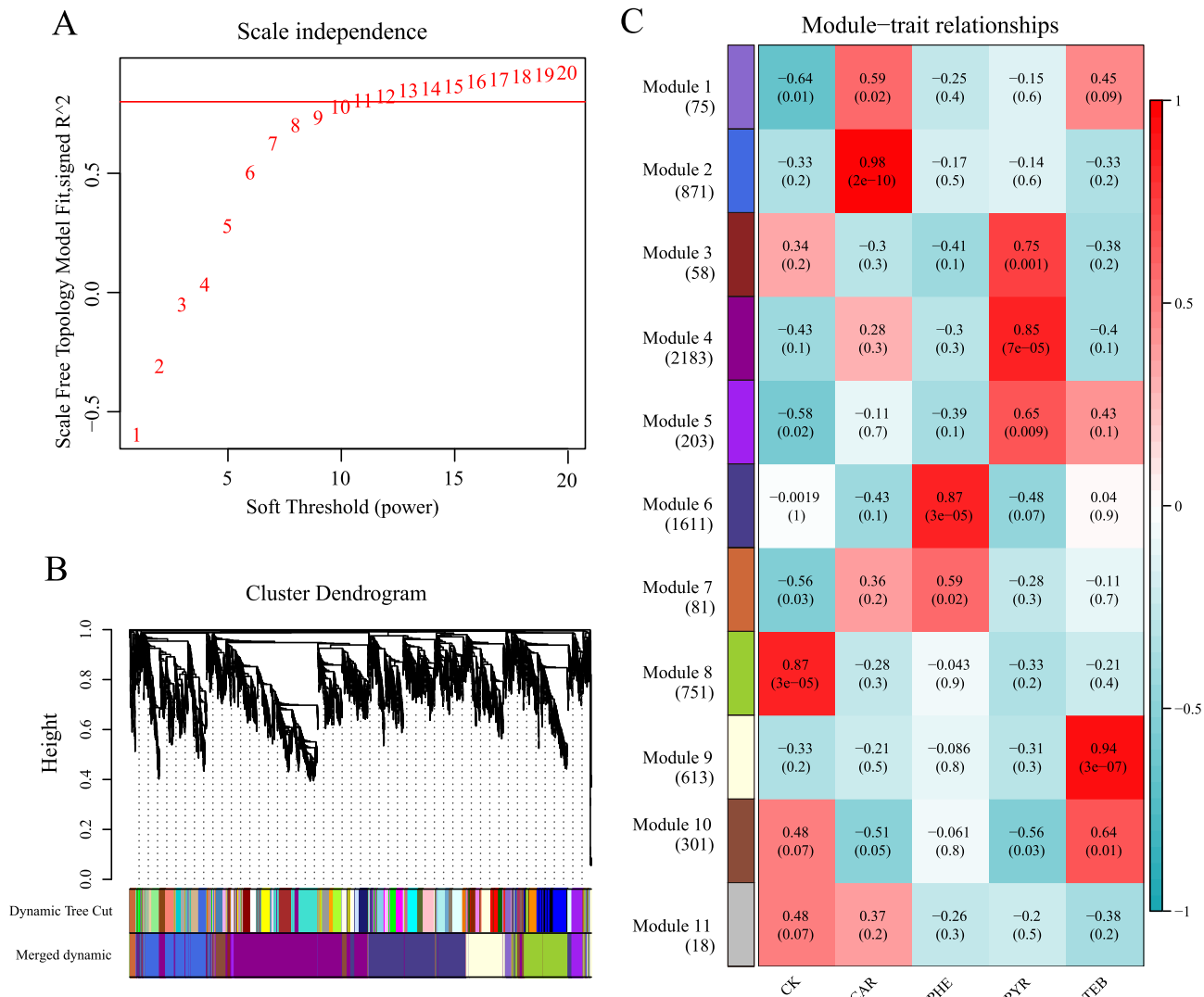


Fig. 7. WGCNA of DEGs from the four comparative groups. (A) Analysis of network topology for various soft-thresholding powers, a soft threshold of 14 was the most optimal value. (B) Clustering dendrogram of all combined DEGs was clustered based on the measurement of dissimilarity. The color band showed the results obtained from the automatic single-block analysis. (C) Heatmap showed the Pearson correlation between the module eigengene and the five groups. The color bar on the right represents the level of correlation from low (blue) to high (red), and the number of DEGs in each module is shown, each cell shows the correlation and the corresponding P value. (For interpretation of the references to color in this figure legend, the reader is referred to the web version of this article.)

and pathways involved in the pathogen's diverse fungicidal resistance.

According to the annotated and enriched results of EggNOG and KEGG databases, the DEGs identified from the four comparisons were mainly involved in carbohydrate and amino acid metabolism (Fig. 3). From this point of view, these effects are similar to the previously reported effects of putrescine treatment [40]. Putrescine, a secondary nitrogen source generated by plants in response to stress and pathogen attack, has been found to have specific effects on *F. graminearum* and its ability to produce the mycotoxin DON [41]. Especially, CAR and PYR treatment seem induce a larger impact on the central carbon metabolism than the other fungicides, as indicated by their enriched GO terms including ATP, carbohydrate, amino acid and cellular lipid metabolic processes (Fig. 2). Interestingly, amino acid biosynthesis and glycolysis metabolism were also reported to be associated with DON production, which are respectively affected by the increased Tri gene transcription and glucose substance [40,42]. In our study, *FGSG_00071* (*Tri1*) was found to be all up-regulated to varying degrees compared to CK treatment, while *FGSG_07896* (*Tri101*) and *FGSG_11025* (*Tri15*) showed the opposite expression. The expression of *FGSG_03543* (*Tri14*), and another protein encoding trichothecene efflux pump *FGSG_03541* (*Tri12*), were

only significantly increased in CAR and PYR group, which might mediate a closer link with the enriched biological function (Table S4). Differences in the expression patterns of these Tri genes require further exploration through functional verification. Additionally, nitrogen metabolism was notably enriched in the PHE treatment group (Fig. 4), aligning with previous KEGG findings in a study on *F. oxysporum* [43]. Previous research has indicated that tebuconazole exerts an inhibitory effect on fungal growth, with the *CYP51* gene in the steroid biosynthesis pathway being a prominent target of tebuconazole [26]. This is also corroborated by our enrichment results of TEB treatment.

The ATP-binding cassette family proteins are widely recognized to be involved in multiple drug resistance in fungi [44,45]. Ycf1 is a type of ABC transporter that helps yeast cells cope with stress by transporting glutathione, a molecule that protects cells from oxidation and metal toxicity, into vacuoles and maintaining the redox balance in the cytoplasm [46,47]. Coincidentally, in our results, only the key ABC transporter *FgYCF1* (*FGSG_05571*) significantly upregulated under all treatments, suggesting its essential role in the resistance to the four fungicides. Heat shock proteins (Hsps) have been reported to be related with many general stress responses rather than thermal stress. Hsp30

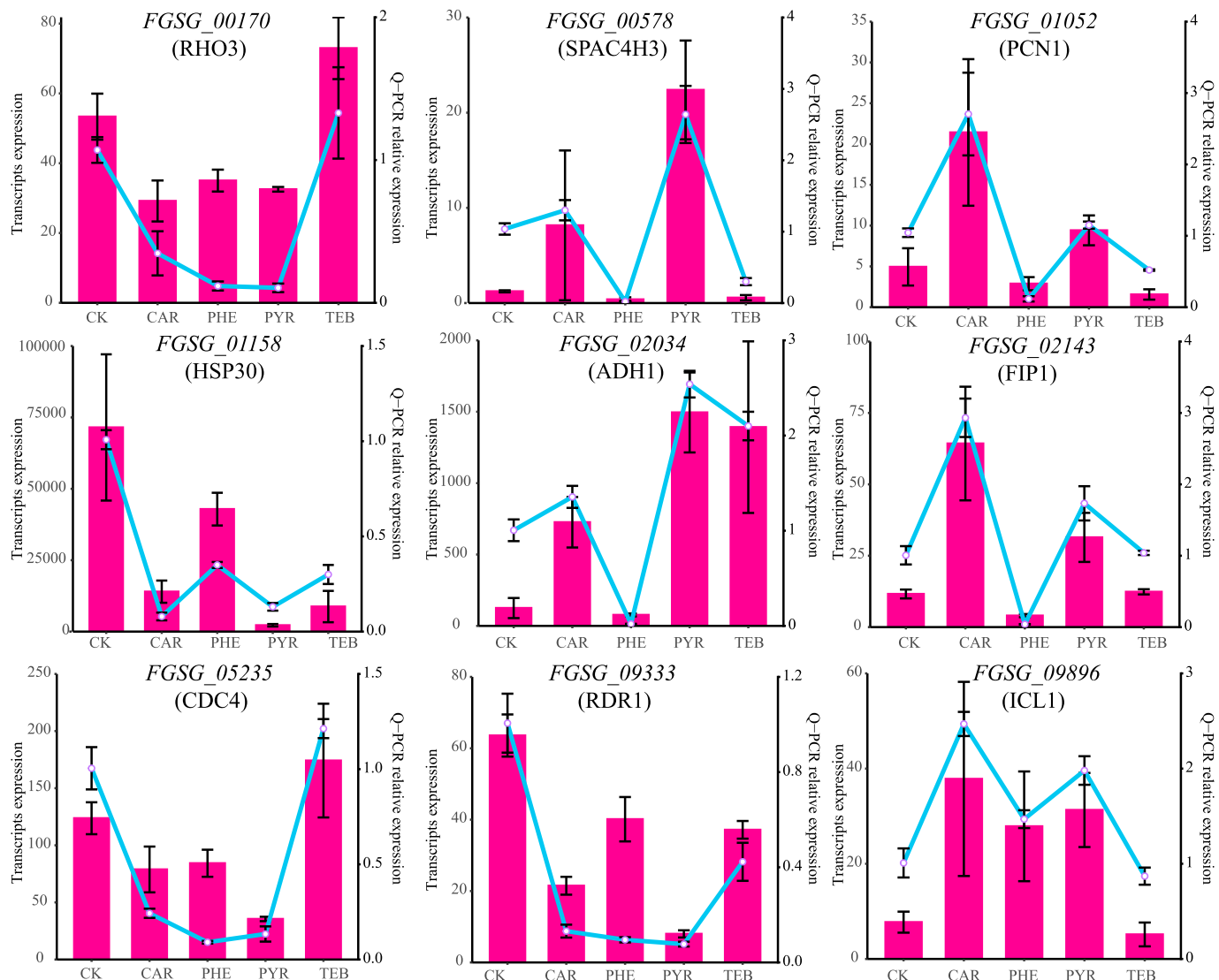


Fig. 8. Verification of the expression patterns of RNA-seq results by qRT-PCR. Nine candidate genes were randomly selected for qRT-PCR analysis. These genes included *FGSG_00170* (Rho3 protein, RHO3), *FGSG_00578* (general stress protein 39, SPAC4H3), *FGSG_01052* (proliferating cell nuclear antigen, PCN1), *FGSG_01158* (30 kDa heat shock protein, HSP30), *FGSG_02034* (alcohol dehydrogenase 1, ADH1), *FGSG_02143* (plasma membrane iron permease, FIP1), *FGSG_05235* (myosin regulatory light chain cdc4, CDC4), *FGSG_09333* (RDR1 protein, RDR1), *FGSG_09896* (isocitrate lyase, ICL1). The bar represents the standard deviations ($\pm SD$) of the mean.

acts as a versatile stress response protein in *Saccharomyces cerevisiae*. Its primary function involves regulating the plasma membrane H⁺-ATPase, promoting cellular homeostasis and energy conservation during stressful conditions [48,49]. Contrary to the trend of *FgYCF1* expression, the expression of *FgHsp30* in the study was significantly reduced in all treatments, suggesting a decline in the defense capability of the pathogen. Another important structural component in the fungi, Chitin synthase D (*FGSG_01949*), also shown a downward trend in each treatment, showing promise to become the important target for the discovery of safe and eco-friendly pesticides, as chitin is an indispensable structural component in insects and fungi, but not in plants and mammals. Certainly, additional ABCs, HSPs and CHSs significantly changed upon at least one fungicide suggested these genes associated with stress response may participate in the process of *F. graminearum* answering multiple fungicide, further confirming the pleiotropic consequences of the exposure to the fungicide.

Given the most obvious metabolic similarity, we focused to the TCA cycle and Glyoxylate and dicarboxylate metabolism in the subsequent functional analysis. Isocitrate lyase (ICL) is a key enzyme in the

glyoxylate cycle, an alternative to the tricarboxylic acid (TCA) cycle. ICL catalyzes the conversion of isocitrate to succinate and glyoxylate, the first step in the glyoxylate bypass. The glyoxylate cycle has been shown to play a crucial role in the virulence of *C. albicans* and *Mycobacterium tuberculosis* [50]. ICL is essential for full virulence in *Magnaporthe grisea*, with elevated expression during infection structure formation. The absence of the glyoxylate cycle impacts the pre-penetration phase, causing delays in germination and infection [51]. In *F. graminearum*, ICL participates in the formation of peritheciun during sexual development [52,53]. Interestingly, the expression patterns of ICL and malate synthase genes differ between in planta and in vitro growth conditions, suggesting a distinction in glyoxylate pathway utilization [54]. In our study, the expression of *FgICL* was prominently up-regulated upon treatment with CAR, PHE and PYR, suggesting an inhibition of the glyoxylate cycle. The observed up-regulation of *FgICL* could indicate an attempt by *F. graminearum* to bypass the blocked TCA cycle and maintain energy production, potentially contributing to fungicide resistance. However, it's important to note that the exact role of *FgICL* in fungicide resistance requires further investigation. This finding is consistent with

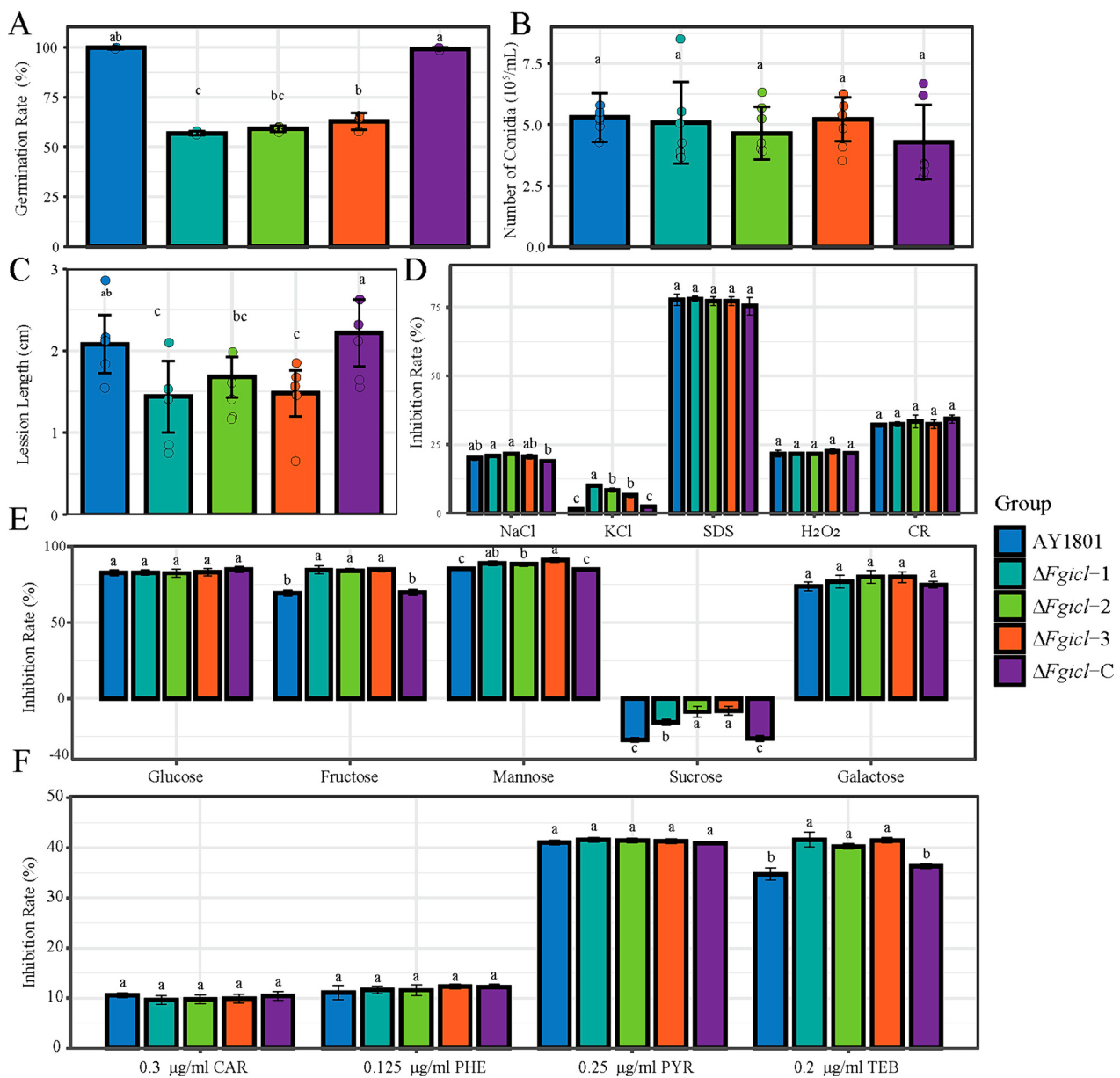


Fig. 9. Functional analysis of *FgICL* gene. (A) Germination rate of wild type and mutants; (B) Sporulation of wild type and mutants; (C) Pathogenicity of wild type and mutants on wheat; (D) Responses of wild type and mutants to different stresses; (E) Utilization of different carbon sources of wild type and mutants; (F) Sensitivity to different fungicides of wild type and mutants.

the notion that fungicides targeting central metabolic pathways can have broad and impactful effects on fungal physiology.

The most abundant soluble carbohydrates, minor components in wheat endosperm, are glucose, fructose, galactose, and sucrose [55]. *Fusarium* infection triggers significant changes in the soluble carbohydrate content of wheat kernels [56]. *F. graminearum* recognizes sucrose molecules, activates *Tri* gene expression and induces trichothecene biosynthesis. However, the levels of trichothecene biosynthesis induced by carbon sources, such as glucose, fructose, lactose, starch and cellulose, have been shown to be strain-specific [57]. The resistance of *F. graminearum* to phenamacril disrupts its capacity to utilize various carbon sources [58]. Similarly, in this study, deletion of *FgICL* gene also affected the ability of *F. graminearum* to use different carbon sources. Interestingly, isocitrate lyase, identified as one of the candidate effector proteins in *F. graminearum* [59] is present in fungi, bacteria, and plants, but the glyoxylate cycle is typically absent in human and animal tissues. This unique difference makes the enzymes attractive targets for selective

antifungal agents.

5. Conclusions

This study presented a comprehensive comparative transcriptomic analysis of *F. graminearum*'s response to four major fungicides. Each fungicide elicited a distinct transcriptomic response and DEGs were primarily associated with carbohydrate and amino acid metabolism. Dynamic clustering and WGCNA identified critical candidate genes related to ATP-binding cassette transporters, heat shock proteins, and chitin synthases, highlighting the fungus' multifaceted response to fungicidal stress. The results revealed that *F. graminearum* employs numerous strategies to overcome fungicide stress, suggesting a pleiotropic antifungal role of fungicides, which is not exclusively associated with growth inhibition. Functional analysis further unveiled the pleiotropic impact of an isocitrate lyase on spore germination, fungal infection, stress response, fungicide sensitivity, and utilization of different

carbon sources in *F. graminearum*. These discoveries could advance the understanding of interaction between fungi and fungicides with different modes of action at transcriptomic level, which in turn could shed light on how resistance might evolve. Furthermore, this research provides valuable insights for developing novel and sustainable strategies to manage Fusarium head blight in cereal crops.

Supplementary data to this article can be found online at <https://doi.org/10.1016/j.ygeno.2024.110869>.

Author statement

All authors have reviewed and approved the final version of the manuscript and agree with its submission to Genomics.

CRediT authorship contribution statement

Xuhao Guo: Writing – review & editing, Writing – original draft, Software, Investigation, Formal analysis. **Kai He:** Writing – review & editing, Writing – original draft, Visualization, Software, Formal analysis. **Mengyu Li:** Validation, Resources, Investigation, Formal analysis, Data curation. **Yuan Zhang:** Visualization, Software, Formal analysis. **Jia Jiang:** Supervision, Methodology, Formal analysis. **Le Qian:** Supervision, Software, Formal analysis. **Xuheng Gao:** Validation, Software. **Chengqi Zhang:** Software. **Shengming Liu:** Supervision, Project administration, Methodology, Funding acquisition, Conceptualization.

Declaration of competing interest

The authors declare that they have no competing interests.

Data availability

The datasets generated and analyzed during the current study are available in Sequence Read Archive (SRA) repository of National Center for Biotechnology Information (NCBI) under accession number PRJNA890947.

Acknowledgements

This research was funded by National Key Research and Development Program of China, grant number 2022YFD1400100; Henan Province Science and Technology Research and Development Plan Joint Fund, grant number 232301420122; Commonwealth Specialized Research Fund of Luoyang, grant number 2302032 A.

References

- [1] R.S. Goswami, H.C. Kistler, Heading for disaster: *fusarium graminearum* on cereal crops, Mol. Plant Pathol. 5 (2004) 515–525.
- [2] M. McMullen, G. Bergstrom, E. De Wolf, R. Dill-Macky, D. Hershman, G. Shaner, D. Van Sanford, A unified effort to fight an enemy of wheat and barley: fusarium head blight, Plant Dis. 96 (2012) 1712–1728.
- [3] N.E. Nnadi, D.A. Carter, Climate change and the emergence of fungal pathogens, PLoS Pathog. 17 (2021) e1009503.
- [4] Y. Chen, H.C. Kistler, Z. Ma, *Fusarium graminearum* Trichothecene mycotoxins: biosynthesis, regulation, and management, Annu. Rev. Phytopathol. 57 (2019) 15–39.
- [5] S. Mishra, S. Srivastava, J. Dewangan, A. Divakar, S. Kumar Rath, Global occurrence of deoxynivalenol in food commodities and exposure risk assessment in humans in the last decade: a survey, Crit. Rev. Food Sci. Nutr. 60 (2020) 1346–1374.
- [6] O. Rocha, K. Ansari, F.M. Doohan, Effects of trichothecene mycotoxins on eukaryotic cells: a review, Food Addit. Contam. 22 (2005) 369–378.
- [7] H.J. Lee, D. Ryu, Worldwide occurrence of mycotoxins in cereals and cereal-derived food products: public health perspectives of their co-occurrence, J. Agric. Food Chem. 65 (2017) 7034–7051.
- [8] Y.J. Zhang, J.J. Yu, Y.N. Zhang, X. Zhang, C.J. Cheng, J.X. Wang, D.W. Hollomon, P.S. Fan, M.G. Zhou, Effect of carbendazim resistance on trichothecene production and aggressiveness of *fusarium graminearum*, Mol. Plant-Microbe Interact. 22 (2009) 1143–1150.
- [9] X.S. Song, X.M. Xiao, K.X. Gu, J. Gao, S.C. Ding, M.G. Zhou, The ASK1 gene regulates the sensitivity of *fusarium graminearum* to carbendazim, conidiation and sexual production by combining with beta2-tubulin, Curr. Genet. 67 (2021) 165–176.
- [10] Z. Zheng, T. Gao, Y. Zhang, Y. Hou, J. Wang, M. Zhou, FgFim, a key protein regulating resistance to the fungicide JS399-19, asexual and sexual development, stress responses and virulence in *fusarium graminearum*, Mol. Plant Pathol. 15 (2014) 488–499.
- [11] Y. Zhu, Y. Zhang, Y. Duan, D. Shi, Y. Hou, X. Song, J. Wang, M. Zhou, Functional roles of alpha1-, alpha2-, beta1-, and beta2-tubulins in vegetative growth, microtubule assembly, and sexual reproduction of *fusarium graminearum*, Appl. Environ. Microbiol. 87 (2021) e0096721.
- [12] L.C. Davidse, Benzimidazole fungicides: mechanism of action and biological impact, Annu. Rev. Phytopathol. 24 (1986) 43–65.
- [13] J. Qiu, T. Huang, J. Xu, C. Bi, C. Chen, M. Zhou, beta-tubulins in *Gibberella zeae*: their characterization and contribution to carbendazim resistance, Pest Manag. Sci. 68 (2012) 1191–1198.
- [14] C. Zhang, Y. Chen, Y. Yin, H.H. Ji, W.B. Shim, Y. Hou, M. Zhou, X.D. Li, Z. Ma, A small molecule species specifically inhibits *fusarium* myosin I, Environ. Microbiol. 17 (2015) 2735–2746.
- [15] N. Liu, S. Wu, D.H. Dawood, G. Tang, C. Zhang, J. Liang, Y. Chen, Z. Ma, The b-ZIP transcription factor FgTfmI is required for the fungicide phenamipacil tolerance and pathogenicity in *fusarium graminearum*, Pest Manag. Sci. 75 (2019) 3312–3322.
- [16] H.J. Liang, Y.L. Di, J.L. Li, H. You, F.X. Zhu, Baseline sensitivity of Pyraclostrobin and toxicity of SHAM to *Sclerotinia sclerotiorum*, Plant Dis. 99 (2015) 267–273.
- [17] H. Ruan, P. Tian, N. Shi, Y. Du, F. Chen, F. Chen, Characterization of pyraclostrobin-resistant *Magnaporthe oryzae*, J. Phytopathol. 170 (2022) 233–241.
- [18] D. Fernandez-Ortuno, F. Chen, G. Schnabel, Resistance to Pyraclostrobin and Boscalid in *Botrytis cinerea* isolates from strawberry fields in the Carolinas, Plant Dis. 96 (2012) 1198–1203.
- [19] R. Becher, U. Hettwer, P. Karlovsky, H.B. Deising, S.G. Wirsel, Adaptation of *fusarium graminearum* to tebuconazole yielded descendants diverging for levels of fitness, fungicide resistance, virulence, and mycotoxin production, Phytopathology 100 (2010) 444–453.
- [20] Y. Yin, X. Liu, B. Li, Z. Ma, Characterization of sterol demethylation inhibitor-resistant isolates of *fusarium asiaticum* and *F. Graminearum* collected from wheat in China, Phytopathology 99 (2009) 487–497.
- [21] H. Qian, J. Du, M. Chi, X. Sun, W. Liang, J. Huang, B. Li, The Y137H mutation in the cytochrome P450 FgCYP51B protein confers reduced sensitivity to tebuconazole in *fusarium graminearum*, Pest Manag. Sci. 74 (2018) 1472–1477.
- [22] C. Zhang, T. Li, L. Xiao, S. Zhou, X. Liu, Characterization of tebuconazole resistance in *Botrytis cinerea* from tomato plants in China, Phytopathol. Res. 2 (2020).
- [23] P. Hellin, R. King, M. Urban, K.E. Hammond-Kosack, A. Legreve, The adaptation of *fusarium culmorum* to DMI fungicides is mediated by major transcriptome modifications in response to azole fungicide, including the overexpression of a PDR transporter (FcABC1), Front. Microbiol. 9 (2018) 1385.
- [24] C.A. Cuomo, U. Gulderen, J.R. Xu, F. Trail, B.G. Turgeon, A. Di Pietro, J.D. Walton, L.J. Ma, S.E. Baker, M. Rep, G. Adam, S. Antoniou, T. Baldwin, S. Calvo, Y.L. Chang, D. Decaprio, L.R. Gale, S. Gnerre, R.S. Goswami, K. Hammond-Kosack, L.J. Harris, K. Hilburn, J.C. Kennell, S. Kroken, J.K. Magnuson, G. Mannhaupt, E. Mauceli, H. W. Mewes, R. Mitterbauer, G. Muehlbauer, M. Munsterkotter, D. Nelson, K. O'Donnell, T. Ouellet, W. Qi, H. Quesneville, M.I. Roncero, K.Y. Seong, I. V. Tetko, M. Urban, C. Waalwijk, T.J. Ward, J. Yao, B.W. Birren, H.C. Kistler, The *fusarium graminearum* genome reveals a link between localized polymorphism and pathogen specialization, Science 317 (2007) 1400–1402.
- [25] Y. Hou, Z. Zheng, S. Xu, C. Chen, M. Zhou, Proteomic analysis of *fusarium graminearum* treated by the fungicide JS399-19, Pestic. Biochem. Physiol. 107 (2013) 86–92.
- [26] X. Liu, J. Jiang, J. Shao, Y. Yin, Z. Ma, Gene transcription profiling of *fusarium graminearum* treated with an azole fungicide tebuconazole, Appl. Microbiol. Biotechnol. 85 (2010) 1105–1114.
- [27] K.Y. Seong, M. Pasquali, X. Zhou, J. Song, K. Hilburn, S. McCormick, Y. Dong, J. R. Xu, H.C. Kistler, Global gene regulation by *fusarium* transcription factors Tri6 and Tri10 reveals adaptations for toxin biosynthesis, Mol. Microbiol. 72 (2009) 354–367.
- [28] J. Bonnighausen, N. Schauer, W. Schafer, J. Bormann, Metabolic profiling of wheat rachis node infection by *fusarium graminearum* - decoding deoxynivalenol-dependent susceptibility, New Phytol. 221 (2019) 459–469.
- [29] R. Becher, F. Weihmann, H.B. Deising, S.G. Wirsel, Development of a novel multiplex DNA microarray for *fusarium graminearum* and analysis of azole fungicide responses, BMC Genomics 12 (2011) 52.
- [30] T. Zhang, Q. Cao, N. Li, D. Liu, Y. Yuan, Transcriptome analysis of fungicide-resistance gene expression profiles in two *Penicillium italicum* strains with different response to the sterol demethylation inhibitor (DMI) fungicide prochloraz, BMC Genomics 21 (2020) 156.
- [31] L. Guo, G. Zhao, J.R. Xu, H.C. Kistler, L. Gao, L.J. Ma, Compartmentalized gene regulatory network of the pathogenic fungus *fusarium graminearum*, New Phytol. 211 (2016) 527–541.
- [32] S. Liu, Z. Che, G. Chen, Multiple-fungicide resistance to carbendazim, diethofencarb, procymidone, and pyrimethanil in field isolates of *Botrytis cinerea* from tomato in Henan Province, China, Crop Prot. 84 (2016) 56–61.
- [33] Y. Chen, A.-F. Zhang, T.-C. Gao, Y. Zhang, W.-X. Wang, K.-J. Ding, L. Chen, Z. Sun, X.-Z. Fang, M.-G. Zhou, Integrated use of Pyraclostrobin and Epoxiconazole for the control of fusarium head blight of wheat in Anhui Province of China, Plant Dis. 96 (2012) 1495–1500.
- [34] D. Kim, B. Langmead, S.L. Salzberg, HISAT: a fast spliced aligner with low memory requirements, Nat. Methods 12 (2015) 357–360.

- [35] M.I. Love, W. Huber, S. Anders, Moderated estimation of fold change and dispersion for RNA-seq data with DESeq2, *Genome Biol.* 15 (2014) 550.
- [36] P. Langfelder, S. Horvath, WGCNA: an R package for weighted correlation network analysis, *BMC Bioinform. 9* (2008) 559.
- [37] M.K. Chaveroche, J.M. Ghigo, C. d'Enfert, A rapid method for efficient gene replacement in the filamentous fungus *aspergillus nidulans*, *Nucleic Acids Res.* 28 (2000) E97.
- [38] J.H. Yu, Z. Hamari, K.H. Han, J.A. Seo, Y. Reyes-Dominguez, C. Scazzocchio, Double-joint PCR: a PCR-based molecular tool for gene manipulations in filamentous fungi, *Fungal Genet. Biol.* 41 (2004) 973–981.
- [39] Z. Hou, C. Xue, Y. Peng, T. Katan, H.C. Kistler, J.R. Xu, A mitogen-activated protein kinase gene (MGV1) in *fusarium graminearum* is required for female fertility, heterokaryon formation, and plant infection, *Mol. Plant-Microbe Interact.* 15 (2002) 1119–1127.
- [40] L. Zhang, X. Zhou, P. Li, Y. Wang, Q. Hu, Y. Shang, Y. Chen, X. Zhu, H. Feng, C. Zhang, Transcriptome profile of *fusarium graminearum* treated by putrescine, *J. Fungi (Basel)* 9 (2022).
- [41] T. Ma, L. Zhang, M. Wang, Y. Li, Y. Jian, L. Wu, H.C. Kistler, Z. Ma, Y. Yin, Plant defense compound triggers mycotoxin synthesis by regulating H2B ub1 and H3K4 me2/3 deposition, *New Phytol.* 232 (2021) 2106–2123.
- [42] T. Shiobara, Y. Nakajima, K. Maeda, M. Akasaka, Y. Kitou, K. Kanamaru, S. Ohsato, T. Kobayashi, T. Nishiuchi, M. Kimura, Identification of amino acids negatively affecting fusarium trichothecene biosynthesis, *Antonie Van Leeuwenhoek* 112 (2019) 471–478.
- [43] Z. Zheng, H. Liu, Y. Shi, Z. Liu, H. Teng, S. Deng, L. Wei, Y. Wang, F. Zhang, Comparative transcriptome analysis reveals the resistance regulation mechanism and fungicidal activity of the fungicide phenamacril in *fusarium oxysporum*, *Sci. Rep.* 12 (2022) 11081.
- [44] G. Dube, N. Kadoo, R. Prashant, Exploring the biological roles of Dothideomycetes ABC proteins: leads from their phylogenetic relationships with functionally-characterized Ascomycetes homologs, *PLoS One* 13 (2018) e0197447.
- [45] N. Khunweeraphong, K. Kuchler, Multidrug resistance in mammals and Fungi—from MDR to PDR: a rocky road from atomic structures to transport mechanisms, *Int. J. Mol. Sci.* 22 (2021).
- [46] N.K. Khandelwal, C.R. Millan, S.I. Zangari, S. Avila, D. Williams, T.M. Thaker, T.M. Tomasiak, The structural basis for regulation of the glutathione transporter Ycf1 by regulatory domain phosphorylation, *Nat. Commun.* 13 (2022) 1278.
- [47] M.S. Szczypka, J.A. Wemmie, W.S. Moye-Rowley, D.J. Thiele, A yeast metal resistance protein similar to human cystic fibrosis transmembrane conductance regulator (CFTR) and multidrug resistance-associated protein, *J. Biol. Chem.* 269 (1994) 22853–22857.
- [48] P.W. Piper, C. Ortiz-Calderon, C. Holyoak, P. Coote, M. Cole, Hsp30, the integral plasma membrane heat shock protein of *Saccharomyces cerevisiae*, is a stress-inducible regulator of plasma membrane H(+)-ATPase, *Cell Stress Chaperones* 2 (1997) 12–24.
- [49] J.P. Burnie, T.L. Carter, S.J. Hodgetts, R.C. Matthews, Fungal heat-shock proteins in human disease, *FEMS Microbiol. Rev.* 30 (2006) 53–88.
- [50] M.F. Dunn, J.A. Ramirez-Trujillo, I. Hernandez-Lucas, Major roles of isocitrate lyase and malate synthase in bacterial and fungal pathogenesis, *Microbiology (Reading)* 155 (2009) 3166–3175.
- [51] Z.Y. Wang, C.R. Thornton, M.J. Kershaw, L. Debao, N.J. Talbot, The glyoxylate cycle is required for temporal regulation of virulence by the plant pathogenic fungus *Magnaporthe grisea*, *Mol. Microbiol.* 47 (2003) 1601–1612.
- [52] S.H. Lee, Y.K. Han, S.H. Yun, Y.W. Lee, Roles of the glyoxylate and methylcitrate cycles in sexual development and virulence in the cereal pathogen *Gibberella zaeae*, *Eukaryot. Cell* 8 (2009) 1155–1164.
- [53] H.K. Kim, S.M. Jo, G.Y. Kim, D.W. Kim, Y.K. Kim, S.H. Yun, A large-scale functional analysis of putative target genes of mating-type loci provides insight into the regulation of sexual development of the cereal pathogen *fusarium graminearum*, *PLoS Genet.* 11 (2015) e1005486.
- [54] J.C. Guenther, H.E. Hallen-Adams, H. Bucking, Y. Shachar-Hill, F. Trail, Triacylglyceride metabolism by *fusarium graminearum* during colonization and sexual development on wheat, *Mol. Plant-Microbe Interact.* 22 (2009) 1492–1503.
- [55] S.A. Ruuska, G.J. Rebetzke, A.F. van Herwaarden, R.A. Richards, N.A. Fettell, L. Tabe, C.L.D. Jenkins, Genotypic variation in water-soluble carbohydrate accumulation in wheat, *Funct. Plant Biol.* 33 (2006) 799–809.
- [56] K. Acs, M. Varga, A. Szekeres, A. Salgo, C. Lantos, F. Bekes, J. Pauk, A. Mesterhazy, Alteration of carbohydrate metabolism in fusarium infected wheat kernels treated with fungicides and its relation to baking technological parameters and Deoxynivalenol contamination, *Agriculture* 13 (2023).
- [57] F. Jiao, A. Kawakami, T. Nakajima, Effects of different carbon sources on trichothecene production and tri gene expression by *fusarium graminearum* in liquid culture, *FEMS Microbiol. Lett.* 285 (2008) 212–219.
- [58] Y. Zhang, W. Chen, W. Shao, J. Wang, C. Lv, H. Ma, C. Chen, Molecular, biological and physiological characterizations of resistance to phenamacril in *fusarium graminearum*, *Plant Pathol.* 66 (2017) 1404–1412.
- [59] M.G. Miltenburg, C. Bonner, S. Hepworth, M. Huang, C. Rampitsch, R. Subramaniam, Proximity-dependent biotinylation identifies a suite of candidate effector proteins from *fusarium graminearum*, *Plant J.* 112 (2022) 369–382.